

## Growth Rate of $\alpha$ -Si:H Film Influenced by Magnetic Field Gradient in MWECR CVD Plasma System\*

Hu Yuehui, Wu Yueying, Chen Guanghua, Wang Qing, Zhang Wenli and Yin Shengyi

(Department of Material Science and Engineering, Beijing University of Technology, Beijing 100022, China)

**Abstract:** The magnetic field profiles, which are produced by three ways in the deposition chamber and plasma chamber of single coil divergent field MWECR CVD system, are investigated. The magnetic field gradient of these magnetic field profiles is obtained quantitatively by using Lorentz fit. The results indicate that the gradient value of the magnetic field profile near by the substrate, which is produced by a coil current with 137.7A if a SmCo permanent magnet is equipped under the substrate holder, is the largest; when the SmCo permanent magnet is taken away, the larger one is produced by the coil current with 137.7A and the smallest one produced by a coil current with 115.2A. High deposition rate of  $\alpha$ -Si:H film is observed near by the substrate with high magnetic field gradient. But uneven deposition rate along the radius of the sample holder is also found by infrared analysis technology when sample is deposited in magnetic field profile, which is produced by the coil current with 137.7A if the SmCo permanent magnet is equipped under the substrate holder.

**Key words:** magnetic field gradient; Lorentz fit;  $\alpha$ -Si:H film; deposition rate; MWECR CVD deposition system

**PACC:** 6140; 6855; 8115H

**CLC number:** TN304.8

**Document code:** A

**Article ID:** 0253-4177(2004)06-0613-07

### 1 Introduction

Researchers were greatly interested in microwave electronic circle resonance chemistry vapor deposition (MWECR CVD) in recent years because of its high electronic density ( $10^{17} \sim 10^{18} \text{ cm}^{-3}$ ) with low gas pressure ( $0.1 \sim 1 \text{ Pa}$ ). So, MWECR CVD system was improved rapidly<sup>[1]</sup>. According to its function and fabrication requirement, various ECR reactors with different levels of complexity have been made. In the research, MWECR CVD system was equipped with a single electromagnetic coil to produce divergent magnetic field with advantages of

simple construction and lower cost. Meanwhile, the ECR generation site of the system was easy to control. However, the ion current density, the electronic temperature, and the potential of plasma strongly depend on the magnetic field gradient<sup>[2]</sup>. It was reported<sup>[3]</sup> that plasma has higher electronic temperature and lower plasma density in a flat magnetic field profiles. This is unfavorable to the hydrogenated amorphous silicon ( $\alpha$ -Si:H) film growth. Since until now no quantitative calculation of the magnetic field gradient has been reported, investigating magnetic field gradient quantitatively is of importance to the deposition of  $\alpha$ -Si:H films. The magnetic field gradients of three different magnetic field profiles in the plasma chamber and de-

\* Project supported by State Key Development Program for Basic Research of China (No. G2000028201)

Hu Yuehui male, was born in 1966, associate professor, PhD candidate. His research interest focuses on amorphous semiconductor thin film. E-mail: 8489023@163.com.

Chen Guanghua male, professor. He is engaged in the research on amorphous semiconductors. Tel: 010-67391876, E-mail: ghchen@bjut.edu.cn

Received 9 October 2003, revised manuscript received 5 January 2004

©2004 The Chinese Institute of Electronics

position chamber have been investigated. The first one was produced by using electromagnetic coil current with 115.2A (the magnetic field profile of type I), the second with  $I = 137.7\text{A}$  (the magnetic field profile of type II), and the third with 137.7A when a SmCo permanent magnet was equipped under the substrate (the magnetic field profile of type III). By the means of Lorentz fit, the quantitative magnetic field gradient as well as its effect on  $\alpha\text{-Si:H}$  film deposition rate were investigated. Uneven deposition rate along the radius of the sample holder was also investigated by infrared analysis technology when sample was deposited in magnetic field profile of type III.

## 2 Experiment

### 2.1 Three kinds of magnetic field profiles

The schematic of divergent field MWECD CVD system with single coil is shown in Fig. 1. The coil was fixed around the plasma chamber. Different coil current produced different magnetic strength and profiles in the plas-

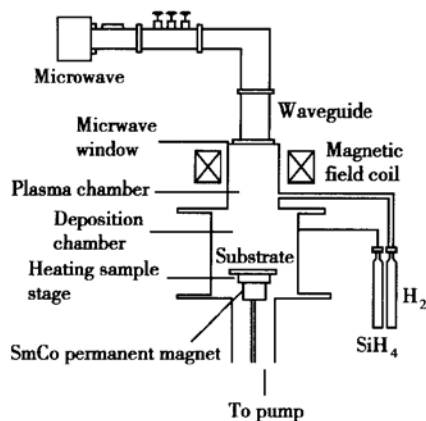


Fig. 1 Schematic of MWECD CVD system

ma chamber and deposition chamber. In room temperature, the magnetic strength in the plasma chamber and deposition chamber was measured by the model TSL-3 Tesla meter, which can measure the axis direction and crosswise direction magnetic field by exchanging the probe<sup>[2]</sup>. As shown in Fig. 1, the SmCo permanent magnet under the substrate holder was equipped in our experiment in order to modify the magnetic field distribution only in the depo-

sition chamber. In this condition, the magnetic field profile of type III shown in Fig. 2 has been obtained at the given  $I = 137.7\text{A}$ . When the SmCo permanent magnet was taken away from the substrate holder below, the magnetic field profiles of type I and II as shown in Fig. 2 have been obtained at the given  $I = 137.7\text{A}$  and  $I = 115.2\text{A}$ , respectively.

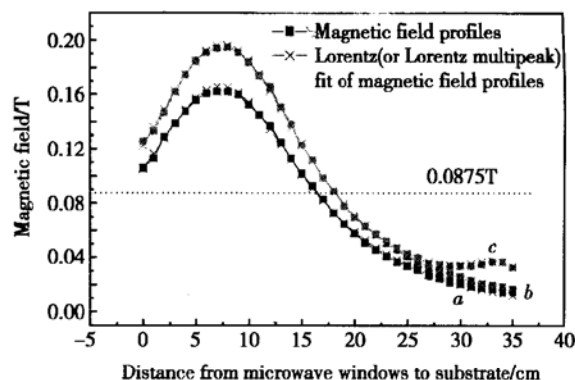


Fig. 2 Lorentz fit of magnetic field profiles (the parameters was shown in Table 2) Curve a: type I magnetic field profile and its Lorentz fit; Curve b: type II magnetic field profile and its Lorentz fit; Curve c: type III magnetic field profile and its Lorentz fit

The SmCo permanent magnet was processed into a cylinder with 6cm diameter and 3cm high by conventional powder metallurgy process method. The magnetic field was measured by DC-flux-integrator at 298K and 423K. Temperature property of remaining magnetization of SmCo permanent magnet is shown in Table 1.

Table 1 Temperature property of remaining magnetization of SmCo permanent magnet

Temperature	298K	423K	298~ 423K
Temperature property of remaining	Br/T	Br/T	$\alpha / (\% \cdot \text{K}^{-1})$
Magnetization	0.016	0.015	- 0.050

Br indicates remaining magnetization; the  $\alpha$  is a temperature coefficient of remaining magnetization.

### 2.2 Fabrication and measurement of $\alpha\text{-Si:H}$ Films

In our experiment, first, substrates (glass, Si wafer) were rinsed and soaked by eluent in order to remove the metal ions. Then, the oil of the substrates was eliminated

by toluene, acetone, and ethanol, and they were soaked in the absolute ethanol to keep in reserve. Finally, they were picked out from the absolute ethanol, dried, and laid on the substrate holder before experiment. The substrates were treated by  $H_2$  plasma for 5min before deposition. Ceramic DC heating furnace capable of controlling the temperature precisely was used to heat the substrates. For thickness measurements, the films were prepared on the glass. Thickness of  $\alpha$ -Si:H were measured by Surf-Com408A Surface Profile Apparatus. For infrared-transmission spectroscopy measurements, the films were prepared on both side of polished Si wafer and measured by Xian-Chinetek FTIR 1020 Fourier spectrometers.

### 3 Results

#### 3.1 Magnetic field profile and magnetic field gradient

Figure 2 shows three types of magnetic field profiles through the central axis ( $z = 0$ ) of both the plasma chamber and deposition chamber. The magnetic field profiles of type I and type II are similar, but their peak sites are different. The former has a peak value in site of 7.3cm; the latter is in site of 7.7cm. Figure 2 also indicates that the ECR position (0.0875T) is 16.5cm for the former and 18cm for the latter. It is clear that the ECR position approaches the microwave window as coil current decreases. The type III begins to present difference in a range from 22.8cm to the substrate comparing with the type II, and this difference maximizes near by the substrate (the distance from microwave to window is 35cm). The Lorentz fit and the magnetic field gradients of three kinds of magnetic field profiles are as follows.

##### 3.1.1 Magnetic field profile of type I and its Lorentz fit curve

Magnetic field gradient was obtained by Lorentz fit with Origin6.1. Curve *a* in Fig. 2 shows the magnetic

field profile of the type I and its Lorentz fit curve. Based on the fit curve formula,

$$y = y_0 + \frac{2A}{\pi} \times \frac{W}{4(x - x_c)^2 + W^2} \quad (1)$$

where  $y_0$  is a baseline offset;  $A$  is the total area under the curve from the baseline;  $x_c$  is the center of the peak;  $W$  is the full width of the peak at half high. The values of fit parameters are shown in Table 2.

Table 2 Values of parameters of Lorentz fit in three kinds of magnetic field profiles

Magnetic field profiles	Fit parameters			
	$y_0$	$x_c$	$W$	$A$
Type I	- 77.7	7.3	20.0	54584.8
Type II	- 86.4	7.5	20.0	64438.1
Type III	- 219	$x_{c1} = 7.5,$	$W_1 = 21.0,$	$A_1 = 71716.2,$
		$x_{c2} = 34.0$	$W_1 = 10.0$	$A_2 = 4546.0$

Relation of magnetic field strength and distance from microwave window to substrate was obtained:

$$y = - 77.7 + \frac{695347.7}{4(x - 7.3)^2 + 400} \quad (2)$$

From Eq. (2), the magnetic field gradient was given:

$$\frac{dy}{dx} = - \frac{5562782(x - 7.3)}{[4(x - 7.3)^2 + 400]^2} \quad (3)$$

##### 3.1.2 Magnetic field profile of type II and its Lorentz fit curve

In the same way, curve *b* in Fig. 2 shows the magnetic field profile of type II and its Lorentz fit curve. Based on Table 2, relation of magnetic field strength and distance from microwave window to substrate was obtained:

$$y = - 86.4 + \frac{820866}{4(x - 7.5)^2 + 400} \quad (4)$$

From Eq. (4), the magnetic field gradient was given:

$$\frac{dy}{dx} = - \frac{6566930(x - 7.5)}{[4(x - 7.5)^2 + 400]^2} \quad (5)$$

##### 3.1.3 Magnetic field profile of type III and its double peaks Lorentz fit curve

Curve *c* in Fig. 2 shows the magnetic field profile of type III and its Lorentz fit curve with double peaks. Based on the fit curve formula:

$$y = y_0 + \frac{2A_1}{\pi} \times \frac{W_1}{4(x - x_{c1})^2 + W_1^2} +$$

$$\frac{2A_2}{\pi} \times \frac{W_2}{4(x - x_{c2})^2 + W_2^2} \tag{6}$$

where  $A_1, A_2$  are the total area of the first and second peak under the curve from the baseline, respectively;  $x_{c1}$  is the center of the first peak;  $x_{c2}$  is the center of the second peak;  $W_1$  is the full width of the first peak at half maximum;  $W_2$  is the full width of the second peak at half maximum.

Based on Table 2, relation of magnetic field strength and distance from microwave window to substrate was obtained as

$$y = -219 + \frac{959258}{4(x - 7.5)^2 + 441} + \frac{28955}{4(x - 34)^2 + 100} \tag{7}$$

The magnetic field gradient was given:

$$\frac{dy}{dx} = -\frac{7674064(x - 7.5)}{[4(x - 7.5)^2 + 441]^2} - \frac{231643(x - 34)}{[4(x - 34)^2 + 100]^2} \tag{8}$$

Based on Eqs. (3), (5), and (8), the gradient of three types of magnetic field profiles were shown in Fig. 3.

The sites of 16.5, 18 (where are the place of 0.0875T of magnetic field profile of type I and type II respectively), and 35cm (where is a place of the substrate), and the gradient of three types of magnetic field profiles are concluded in Table 3.

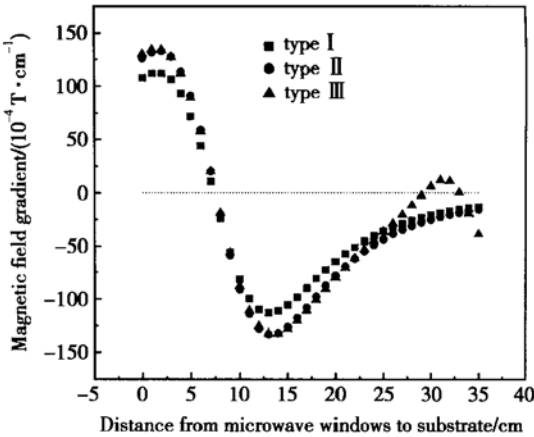


Fig. 3 Distribution of magnetic field gradient

Table 3 Magnetic field gradient of three kinds of magnetic field profiles through the central axis ( $z = 0$ ) of both plasma chamber and deposition chamber

Position/ cm	Magnetic field gradient of three kinds of magnetic field profiles/( $10^{-4}T \cdot cm^{-1}$ )		
	Type I	Type II	Type III
16	- 105.5	- 126.9	- 127.9
18	- 89.5	- 107.7	- 110.8
35	- 12.8	- 15.4	- 38.9
29			- 1.05
33			- 0.09

In Fig. 3, it also indicates that there are two sites of 29cm and 33cm where the gradients of magnetic field profile of type III have small values shown in Table 3. Table 4 shows the distribution of magnetic field gradient along the axis and magnetic field strength along the crosswise near by the sample holder from radius.

Table 4 Distribution of magnetic field gradient along the axis direction and magnetic field strength along the crosswise near by the sample holder from radius

Radius of the sample holder/ cm	Magnetic field profiles					
	Magnetic field gradient along the axis direction in three kinds of magnetic field profiles / ( $10^{-4}T \cdot cm^{-1}$ )			Magnetic field strength along the crosswise direction in three kinds of magnetic field profiles / $10^{-4}T$		
	Type I	Type II	Type III	Type I	Type II	Type III
0	- 12.8	- 15.4	- 38.9	140	160	286
1	- 12.6	- 15.5	- 37.1	130	150	303
2	- 12.0	- 14.2	- 15.0	120	150	303
3	- 11.8	- 14.0		110	150	300
4	- 11.1	- 13.4	- 16.6	110	140	290

### 3.2 Deposition rate of $\alpha$ -Si:H film

Figure 4 presents the results of deposition rate of  $\alpha$ -Si:H films in three types of magnetic field profiles. Deposition conditions of films were given in Table 5. The substrate temperature was set in 54, 100, 140, 170, and 210 °C successively. As shown in Fig. 4, the deposition rate generally trends to decrease as the temperature increases. Under the condition of magnetic field profile of type III, the deposition rate of  $\alpha$ -Si:H film is the largest. The larger one and the smallest one are of type II and type I, respectively.

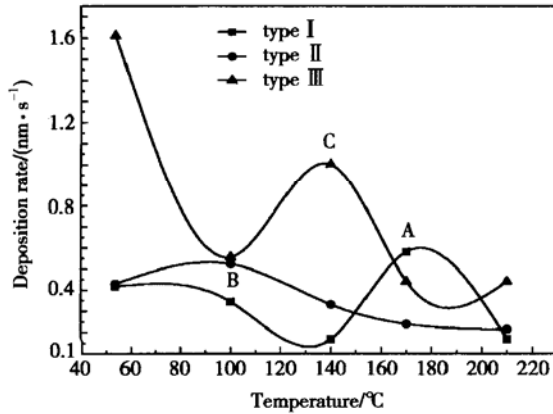


Fig. 4 Deposition rate versus temperature

Table 5 Deposition condition

Power	240W
SiH <sub>4</sub> /H <sub>2</sub> (ratio of mass)	20%
Total flux of gas source	20sccm
Back pressure	0.4Pa
Reaction pressure	1Pa
Distance from microwave window to substrate	35cm

## 4 Discussion

### 4.1 Reason of magnetic field gradient influencing deposition rate of $\alpha$ -Si:H film

The reason that the growth rate of  $\alpha$ -Si:H films is different in different magnetic field profiles is as follows. The plasma introduced from ECR zone drifts down along  $z$  axis, which is the direction of the magnetic field gradient decrease. The drift rate  $V_z$  can be expressed by the formula<sup>[4]</sup>:

$$V_z = \left(\frac{kT_e}{2}\right)^{1/4} \frac{1}{K_e m_e^{3/4}} \left[ - \left(\frac{\partial B_z}{\partial z}\right)_r \right]^{1/2} (rz)^{1/2} \quad (9)$$

where the  $K_e$  is electron mobility,  $\left(\frac{\partial B_z}{\partial z}\right)_r$  is  $z$  axis magnetic field gradient,  $k$  is Boltzman constant,  $T_e$  is electron temperature,  $m_e$  is electron mass,  $r$  and  $z$  the sites of coordinate. Based on Eq. (9), under the same condition, near by the substrate, the larger of the magnetic field gradient value is, the larger of the drift rate  $V_z$  is. In Table 3, near by the substrate (the distance from microwave window to the substrate is 35cm), the gradient of the magnetic field profile of type III is the largest. So its plasma drift rate and plasma density in the deposition chamber are both the largest. The larger and the smallest  $v_s$  and their plasma density in the deposition chamber are in the condition of the magnetic field profile of type II and type I, respectively. We assume that the larger of  $v_s$  and plasma density in the deposition chamber are, the higher of the flux of SiH<sub>3</sub> radicals per surface site is. In MGP model<sup>[5]</sup>, SiH<sub>3</sub> is assumed to the only growth precursor. Therefore, direct abstraction of surface H probability  $p_{ab}$  is high. The relation of the direct abstraction of surface H probability  $p_{ab}$ , direct sticking of surface dangling-bond probability  $p_s$ , and fractional dangling-bond coverage  $\theta_{db}$  is expressed as

$$\theta_{db} = \frac{1}{1 + p_s/p_{ab}} \quad (10)$$

Based on the Eq. (10), if  $p_s$  is an invariable value, the higher of the direct abstraction of surface H probability  $p_{ab}$  is, and the larger of the fractional dangling-bond coverage  $\theta_{db}$  is. This is benefit for the film growth. It is the reason that the deposition rate is high under the condition of high magnetic field gradient found in our experiment.

### 4.2 Relation of deposition rate to temperature

The relation of deposition rate to temperature is shown in Fig. 4. The dots of A, B, and C in Fig. 4 are assumed errors of different samples in the experiment. Thus the deposition rate generally trend to decrease monotonically as the temperature increases. This result agrees with Kobayashi<sup>[6]</sup>. The reasons of the errors will be investigated in our further work.

In Fig. 4, it was found that the growth rate deposited

in the magnetic field profile of type III is close to that of type II at the temperature above 180 °C. Based on the results of Table 1, we consider that this phenomenon is resulted from demagnetization of the SmCo permanent magnet.

### 4.3 Unevenness of deposition rate

As shown in Table 4, the unevenness of crosswise direction magnetic field is unobvious in three magnetic field profiles, but that property of  $z$  axis direction is notable along the radius of the sample holder in the magnetic field profile of type III. Based on the discussion from section 4.1, we assumed that its unevenness of deposition rate is

the most obvious, which will result in the unevenness of thickness and microstructure of sample. In order to prove this, the samples of  $\alpha$ -Si:H films deposited in the magnetic field profiles of type II and type III at 54 °C and 140 °C were investigated by the infrared absorption spectra technology<sup>[7,8]</sup>. In Fig. 5, we can see that the spectra of sample of  $\alpha$ -Si:H films deposited in magnetic field profile of type III show broader peaks obviously than that of type II at the same temperature. Langford *et al.*<sup>[9]</sup> considered that these broader peaks imply that the amorphous network is more disordered and its microvoid density of internal surface increases. This result agrees with our assumption of above.

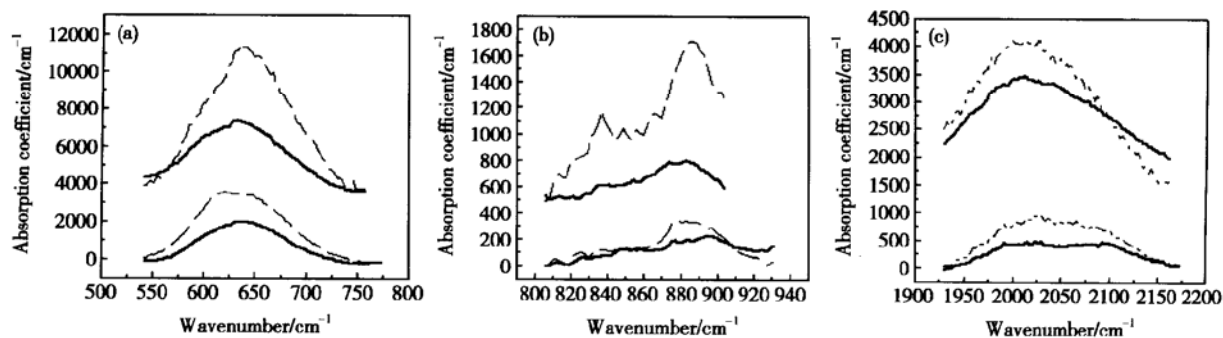


Fig. 5 Absorption spectra of  $\alpha$ -Si:H films deposition in magnetic field of type III (solid lines) and type II (dashed lines) in the wagging (a), bending (b), and stretching-mode regions (c). Spectra are shown in pairs to compare uneven features for sample with temperature in magnetic field profile of type III and type II. From bottom to top, the temperature is 54 °C and 140 °C.

## 5 Conclusion

The magnetic field profile in the deposition chamber and plasma chamber of single coil divergent field MWECD CVD system was modified by different coil current or by equipping the SmCo permanent magnet under the substrate holder. It was found that ECR zone moves up to the microwave window as coil current decreases. The gradients of these magnetic field profiles were obtained by using Lorentz fit, in which near by the substrate type III is the

largest, type II is second, and type I is the smallest. It was also found that the effect of the magnetic field gradient on deposition rate of  $\alpha$ -Si:H film is very obvious. The larger the magnetic field gradient value is, the higher of the growth rate is. Meanwhile, the unevenness of deposition rate of sample deposited in the magnetic field profile of type III investigated by the infrared absorption spectra technology is the most obvious, which is unfavorable to the  $\alpha$ -Si:H films uniform. To overcome this problem is our work in the future.

## References

- [ 1 ] Asmussen J Jr, Grotjohn T A. The design and application of electron cyclotron resonance discharges. *IEEE Trans Plasma Sci*, 1997, 25( 6 ): 1196
- [ 2 ] Samukawa S, Nakamura T. Dependence of electron cyclotron resonance plasma characteristics on magnetic field profiles. *Jpn J Appl Phys*, 1991, 30( 11B ): 3147
- [ 3 ] Vargheese K D, Rao G M. Electrical properties of silicon nitride films prepared by electron cyclotron resonance assisted sputter deposition. *J Vac Sci Technol A*, 2001, 19( 5 ): 2122
- [ 4 ] Dole T, Holber W, Kimura S. Basic chemistry and mechanisms of plasma etching. *J Phys Soc Jpn*, 1982, 51( 2 ): 286
- [ 5 ] Kessels W M M, Smets A H M, Marra D C. On the growth mechanism of  $\alpha$ -Si:H. *Thin Solid Films*, 2001, 383( 1/2 ): 154
- [ 6 ] Kobayashi K, Hayam M, Kawamoto S. Characteristics of hydrogenated amorphous silicon films prepared by electron cyclotron resonance microwave plasma chemical vapor deposition method and their application to photodiodes. *Jpn J Appl Phys*, 1987, 26( 2 ): 202
- [ 7 ] Manfredotti C, Fizzotti F, Boero M, et al. Influence of hydrogen-bonding configurations on the physical properties of hydrogenated amorphous silicon. *Phys Rev*, 1994, B50( 24 ): 18046
- [ 8 ] Maley N. Critical investigation of the infrared-transmission data analysis of hydrogenated amorphous silicon alloys. *Phys Rev*, 1992, B46( 4 ): 2078
- [ 9 ] Langford A A, Fleet M L, Nelson B P, et al. Infrared absorption strength and hydrogen content of hydrogenated amorphous silicon. *Phys Rev*, 1992, B45( 23 ): 13367

MWECD CVD 系统中磁场梯度对  $\alpha$ -Si:H 薄膜沉积速率的影响\*

胡跃辉 吴越颖 陈光华 王 青 张文理 阴生毅

(北京工业大学材料学院, 北京 100022)

**摘要:** 为了定量地得到磁场梯度对  $\alpha$ -Si:H 薄膜沉积速率的影响, 对单磁场线圈分散场 MWECD CVD 系统等离子体室和沉积室中用三种方法得到的磁场形貌进行了研究. 通过洛伦兹拟合的方法定量地得到了这些磁场形貌的磁场梯度. 结果表明, 样品台下面放置钕钴永磁体并使磁场线圈电流为 137.7A 时其衬底附近磁场梯度值最大, 样品台下面无钕钴永磁体时, 磁场线圈电流分别为 137.7A 和 115.2A 的磁场梯度值依次为次之和最小. 制备  $\alpha$ -Si:H 薄膜时, 在衬底附近具有高的磁场梯度值可以得到高的沉积速率. 通过红外吸收谱技术分析, 虽然样品台下面放置钕钴永磁体并使磁场线圈电流为 137.7A 下能得到最大的沉积速率, 但是沿样品台半径方向沉积速率呈现很明显的不均匀分布.

**关键词:** 磁场梯度; 洛伦兹拟合;  $\alpha$ -Si:H 薄膜; 沉积速率; MWECD CVD 沉积系统

**PACC:** 6140; 6855; 8115H

**中图分类号:** TN304.8

**文献标识码:** A

**文章编号:** 0253-4177(2004)06-0613-07

\* 国家重点基础研究发展规划资助项目(批准号: G2000028201)

胡跃辉 男, 1966 年出生, 副教授, 博士研究生, 主要从事非晶硅薄膜的研究.

陈光华 男, 教授, 主要从事非晶半导体的研究.

2003-10-09 收到, 2004-01-05 定稿